International Journal of Biological Macromolecules 78 (2015) 23–31

Contents lists available at ScienceDirect

International Journal of Biological Macromolecules

journal homepage: www.elsevier.com/locate/ijbiomac

Tough and highly stretchable polyacrylamide nanocomposite hydrogels with chitin nanocrystals

Mingxian Liu*, Jiandong Huang, Binghong Luo, Changren Zhou*

Department of Materials Science and Engineering, Jinan University, Guangzhou 510632, PR China

ARTICLE INFO

Article history:
Received 5 March 2015
Received in revised form 20 March 2015
Accepted 25 March 2015
Available online 2 April 2015

Keywords:
Toughness
Swelling
Interfacial interactions

ABSTRACT

Chitin nanocrystals (CNCs) that were 10–20 nm wide and 100–500 nm long were synthetized via acidolysis and characterized with various methods. To avoid the flocculation of CNCs in the initiator solution during acrylamide polymerization, chitosan was selected as a surface modifier. The chitosan-modified CNCs were employed as multifunctional crosslinkers for the polyacrylamide (PAAm) nanocomposite (NC) hydrogels. The NC gels were tough and stretchable; for example, the maximum tensile strength and the elongation at break of the NC gels were 90 kPa and 3070%, respectively. The dynamic shear modulus of the NC gels was also significantly higher than that of the PAAm. The NC gels were nearly free of residual strain after 2000% elongation. The microstructures of all NC gels were porous, with a pore size of 20–100 μm. The maximum equilibrium swelling degree of the NC gels was 3800%. The improvement in the properties of the NC gels is attributed to the good dispersion of CNCs and the interfacial interactions in the composites. This work developed PAAm NC hydrogels with CNCs for application as absorbent or biomedical material due to the high mechanical properties, high absorb ability and good biocompatibility of CNCs and explored new applications for CNCs as well.

1. Introduction

Chitin, a structural polymer in shellfish, insects, and microorganisms, is the second most abundant natural polysaccharide after cellulose. The amorphous domains of chitin can be removed by acidolysis to produce nanoscale crystallites known as chitin nanocrystals (CNCs) [1]. CNCs exhibit a rod-like morphology with an average length of 100–500 nm and a diameter of 10–25 nm depending on the chitin source and reaction conditions. CNCs are characterized by many features, such as a high mechanical strength (the longitudinal and transverse moduli are 150 and 15 GPa, respectively), large aspect ratio, easy availability, nontoxicity, biodegradability, and low density [2]. Various functional groups of CNCs, such as hydroxyl groups and amide groups, facilitate surface modifications. As nanoparticles derived from a renewable source, CNCs have attracted attention from both the academic and industrial fields in the recent years [3,4]. CNCs have extensive applications in many fields, such as polymer composite manufacturing, the cosmetic industry, the food industry (where they serve as additives), drug delivery, and tissue engineering.

As polymer nanofillers, CNCs are good substitutes for inorganic nanoparticles for reinforcing various types of polymers. For example, rubber-CNC nanocomposites have been prepared from a mixed suspension of CNCs and rubber latex [5–7]. This method was further extended to carboxylated styrene butadiene rubber (SBR)-CNCs nanocomposites [8]. CNCs can significantly increase the tensile strength and modulus of the rubber matrix, which is attributed to the formation of rigid three-dimensional networks that result from interactions between the components, such as hydrogen bonds that form between the nanocrystals. CNCs can also reinforce thermoplastic polymers, such as poly(styrene-co-butyl acrylate), polyurethane [9], and soy protein isolate (SPI) [10,11]. Furthermore, CNCs are preferred to other nanofillers such as carbon nanotubes for preparing water soluble polymer nanocomposites due to their hydrophilicity. Chitosan [12], polyvinyl alcohol [13,14], cellulose [15], and silk fibroin [16] composites containing CNCs have been successfully prepared. CNCs can promote cell spreading on the polymer matrix; thus, these composites have potential applications as tissue engineering scaffolds. However, the preparation and application of CNCs have not been as extensively researched and developed in reinforcing polymers in the form of hydrogel as cellulose nanocrystals [17,18]. Therefore, the development of polymer nanocomposites based on CNCs is of strategic importance because of the abundant availability and special properties of CNCs.

* Corresponding authors. Tel.: +86 20 8522 3279; fax: +86 20 8522 3271.
E-mail addresses: liumx@jnu.edu.cn (M. Liu), tcrz9@jnu.edu.cn (C. Zhou).

http://dx.doi.org/10.1016/j.ijbiomac.2015.03.059
0141-8130/

Nanocomposite (NC) gels consisting of organic polymer and nanoparticles were first proposed by Haraguchi et al. [19]. The nanoparticles act as the physical crosslinking points for the polymer chains [20–22]. NC gels feature superior optical transparency, tensile extensibility (~2000%), swelling ratio and sensitivity to stimuli compared to polymers that are crosslinked via covalent bonds [20]. Various nanoparticles, including nanoclays [23,24], carbon nanostructures [25], and cellulose nanocrystals [26,27], have been employed as the reinforcing component of NC gels. For example, graphene oxide (GO) and polyacrylamide (PAAm) can form an organic/inorganic hybrid network hydrogels via hydrogen bonding, ionic bonding, and physical adsorption [28]. Halloysite nanotubes (HNTs) can also strongly interact with PAAm, leading to high-performance NC gels [29]. Considering the unique structural features of CNCs, exploring the feasibility of preparing PAAm NC gels with CNCs is theoretically and practically important. Since the primary component is water, NC gels can be utilized as environmentally friendly rubbery materials in the management of resources and waste, drug delivery systems, wound dressing, and smart devices.

In the present work, CNCs were prepared by acidolysis and were subsequently characterized. To control their surface potential, chitosan was added to the CNC suspension to prevent their flocculation in the initiator aqueous solution (potassium persulfate) during acrylamide polymerization. The mechanical, morphological, rheological, and swelling properties of the PAAm-CNCs NC gels were systematically investigated. The PAAm-CNCs NC gels were tougher and longer at the breaking point during tensile testing than the nanoclay-based NC gels. Furthermore, PAAm-CNCs NC gels constitute a novel composite system that combines the advantages of CNCs, such as their biodegradability, low cost, "green" character and availability in nature, with the ability of acrylamide monomers to readily form a gel. Moreover, PAAm NC gels containing CNCs are preferred over gels containing cellulose nanocrystals or nanoclay because they disperse well in an aqueous solution and are biocompatible. Therefore, the prepared NC gels have potential applications in waste treatment and drug delivery.

2. Experimental

2.1. Materials

Chitin powder (K1262) was purchased from Sanland-Chem International Inc. and used without further purification. The degree of N-acetylation (DA) of the chitin was 0.98. Chitosan (CS) was purchased from Jinan Haidebei Marine Bioengineering Co. Ltd (China). Its deacetylation and viscosity-average molecular weight were 95% and 600,000 g/mol, respectively. Acrylamide (AM) was purchased from Tianjin Damao Chemical Reagent Factory (China) and recrystallized from a hexane/toluene mixture. Potassium peroxydisulfate ($K_2S_2O_8$, KPS) was of analytical reagent grade and recrystallized from deionized water. Pure water was produced by deionization and filtration with a Millipore purification apparatus (resistivity > 18.2 MΩ cm) and bubbled with nitrogen gas for more than 1 h prior to use.

2.2. Preparation of chitin nanocrystals

Chitin nanocrystals (CNCs) were prepared according to a previous report with slight modification [6]. Chitin (0.033 g/mL) was hydrolysed in 3 N HCl at 105 °C for 3 h under stirring. After acid hydrolysis, the suspensions were diluted with distilled water followed by centrifugation (10,000 rpm/min for 5 min). This process was repeated three times. Next, the suspensions were transferred to dialysis bags and dialysed for 24 h against distilled water until pH = 6. The dispersion of nanocrystals was completed by a further 2.5 min ultrasonic treatment for every 40-mL aliquot. The suspensions were then freeze-dried, and the CNC powder was stored in a desiccator.

2.3. Synthesis of PAAm-CNCs NC gels

The NC gels were prepared via the in situ free-radical polymerization of AM in the CNC aqueous suspension. The CNC suspensions were prepared by treating freeze-dried CNCs powder with ultrasound using a JY99-IIDN ultrasonic cell crusher (Ningbo Scientz Biotechnology Co., Ltd., China). The suspensions were colloidal and highly stable. Upon adding the initiator KPS solution, the nanocrystals immediately coagulated due to a change in charge. To address this problem, a positively charged chitosan acidic aqueous solution (1% (w/v), pH = ~4.0) was added into the CNC suspensions to further increase its positive charge. The typical NC gel synthesis procedure was similar a previously published protocol [20]. Three grams of AM was added to 20 mL of aqueous CNC suspension, and the resultant mixture was stirred for 30 min at room temperature. The solutions were bubbled with nitrogen gas for 20 min to replace the oxygen gas in the systems. Finally, 3 mL of 20 wt.% KPS solution was added to the system under stirring for 5 min. The mixed solutions were then cast into glass tubes with a diameter of 7 mm. The polymerization was carried out in a vacuum oven at 65 °C for 18 h. The sample details and their abbreviations used in this study are listed in Table 1. The neat PAAm linear polymer was prepared in manner similar to that used to prepare the NC gels, but without the addition of CNCs. The PAAm composite hydrogels containing raw CNCs (PW) or chitosan (PC) were also prepared using a similar procedure in order to compare the properties.

2.4. Characterization of the CNCs and its interactions with chitosan

2.4.1. Scanning electron microscopy (SEM)

The SEM images were obtained with a Philips LEO1530 VP SEM machine. A dilute aqueous CNC suspension (0.005 wt.%) was dropped onto glass slides, which were then dried at room temperature. The voltage of the electron beam used for SEM observation was 5 kV.

2.4.2. Transmission electron microscopy (TEM)

A transmission electron microscopy (TEM) analysis of CNCs was carried out with a Philips Tecnai 10 TEM. A dilute aqueous CNC suspension was dropped onto a carbon-coated copper grid, which was then dried. The accelerating voltage for the TEM observation was 100 kV.

2.4.3. Atomic force microscopy (AFM)

A multimode AFM with a NanoScope IIIa controller (Veeco Instruments) was used to evaluate the surface morphology of CNCs. A dilute CNC suspension (0.005 wt.%) was dispersed and dried on a piece of freshly cleaved mica, and the images were collected under

Table 1
Chemical composition for preparation of the hydrogels.

Samples	AM (g)	KPS (g)	H_2O (mL)	CNCs (g)	CS (g)
PAAm	3	0.06	20	0	0
PW	3	0.06	20	0.08	0
PC	3	0.06	20	0	0.08
PWC	3	0.06	20	0.08	0.08
$PW_{1.875}C$	3	0.06	20	0.15	0.08

contact mode using a soft cantilever (NP-S20, Veeco, force constant ca. 0.1 nN/nm).

2.4.4. X-ray diffraction (XRD)

The XRD profiles of the freeze-dried CNC powder were obtained using an X-ray diffractometer (Rigaku, MiniFlex600, Cu Kα, Japan) at room temperature. The scanning angle ranged from 5° to 60°.

2.4.5. ξ-Potential characterization

The zeta potentials of dilute CNCs, chitosan–CNC (1:1 weight ratio) suspensions, and chitosan-CNCs in KPS solution were measured using a Zetasizer Nano ZS (Malvern Ltd., UK). Prior to each measurement, the operating conditions were checked and adjusted using a calibrated latex dispersion supplied by the instrument manufacturer (zeta potential -50 ± 5 mV).

2.5. Characterization of the PAAm-CNCs NC gels

2.5.1. Mechanical properties determinations

The tensile testing of PAAm-CNCs NC gels was carried out using a SHIMADZU AG-1 machine at 25 °C. The samples for tensile testing were rod-like in shape with a diameter of 7 mm. The crosshead speed was 100 mm/min. The stress–strain curves for the elongation–recovery of the PWC (PAAm + CNCs + chitosan) NC gels were obtained by stretching the samples to 1000% and 2000% strain and allowing them to revert at the same speed (100 mm/min). The hysteresis in the stress–strain curve was recorded.

2.5.2. Rheological property measurements

The rheological properties of linear PAAm and NC gels were measured with a Kinexus rotational rheometer (Malvern Instruments Ltd.) using parallel plates that were 20 mm in diameter at 25 ± 0.5 °C. The gap between the two parallel plates was set to 1 mm. First, a dynamic strain sweep from 0.1% to 100% was carried out at an angular frequency of 1 Hz, followed by a frequency sweep from 0.1 to 100 Hz at a fixed strain of 0.5%.

2.5.3. Scanning electron microscopy (SEM)

The fractured surfaces of the freeze-dried gel samples were plated with a thin layer of gold prior to the SEM observations on a HITACHI TM3030 SEM machine. The voltage of the electron beam used for SEM observation was 5 kV.

2.5.4. Swelling experiments

Swelling experiments for all samples were performed at room temperature by immersing the prepared or naturally dried NC gels in an excess of pure water at room temperature and changing the water several times. The weight change of the swollen gel was recorded over time. The equilibrium percentage degree of swelling (EDS) was calculated as follows:

$$\mathrm{EDS}\,(\%) = \frac{W_s - W_d}{W_d} \times 100\%$$

where W_s is the weight of the swollen gel, and W_d is the weight of the corresponding dried gel.

2.5.5. Data analysis

In all the experiments, a minimum of five samples was used. Obtained values in each experiment were normalized with the control samples. Results are expressed as the means of at least five replicates ± SD (standard deviation). Statistical analysis was performed using the one-way analysis of variance (ANOVA) with 95% confidence interval.

3. Results and discussion

3.1. Characterization of CNCs

The chitin aqueous suspension was treated with strong ultrasound (800 W × 1 h) to completely exfoliate the bundled chitin microfiber prepared by acidolysis [30]. Fig. 1 shows the appearance of the CNC suspension before and after ultrasonic treatment. The suspension of CNCs became a clear and colourless colloidal solution after ultrasonic treatment. The ultrasonic treatment could disintegrate the bundles of chitin microfibers into nanofibers by destroying the hydrogen bonds and overcoming the Van der Waals forces [31,32]. The high stability of CNCs in the aqueous suspensions is due to the electrostatic repulsion that results from the protonation of acetyl groups. The morphology of CNCs was observed using SEM, TEM, and AFM (Fig. 2). The CNCs were 10–20 nm wide and 100–500 nm long. The high aspect ratio of CNCs allows them to act as nanofillers to reinforce polymers. The widths, lengths and aspect ratios of the CNCs have already been reported in detail in previous papers [31,33], and similar results were obtained in this study. The XRD pattern of CNCs exhibited strong scattering peaks at 2θ angles of 9.6° and 19.5°, as well as three other peaks at ~21°, 23° and 26° (Fig. 3). These peaks are consistent with the diffraction peaks of α-chitin [12,34], indicating that the acidiolysis process does not affect the apparent degree of chitin crystallinity.

3.2. Interactions between CNCs with chitosan

The stability of aqueous CNCs suspension is mainly contributed by their hydrophilicity and electrostatic repulsion of positively-charged acetyl groups. Even though, the contribution is not strong enough to resist an increase of ion strength, because of the screen effect of ions to the electrostatic field. A example for breaking the stability of the nanoparticles by the salt ions is that NaCl makes graphene oxide sheets aggregate in the aqueous dispersion [35]. The acrylamide and the initiator (KPS) were successively added to the CNC suspension to prepare the PAAm-CNCs hydrogels. The CNCs immediately flocculated when KPS was added to the CNC suspension (Fig. 4(b)). KPS is a salt which can dissociate into positively and negatively charged ions in aqueous solution. The KPS attracted the CNCs can weaken the interactions between the nanocrystals. As a result, the addition of KPS leads to the significant aggregation of CNCs, which hinders the preparation of NC gels that contain homogenously distributed CNCs. Therefore, surface of the CNCs needs to be modified to prepare polyacrylamide hydrogels. To address this problem, positively charged chitosan was first added to the CNC suspension, which could effectively prevent the flocculation of CNCs upon the addition of KPS. This effect is

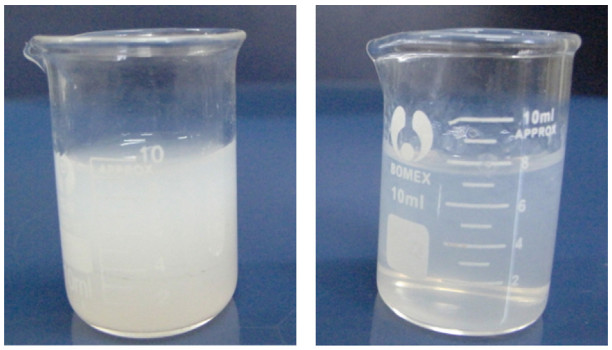

Fig. 1. The appearance of CNCs suspension before (a) and after (b) ultrasonic treatment.

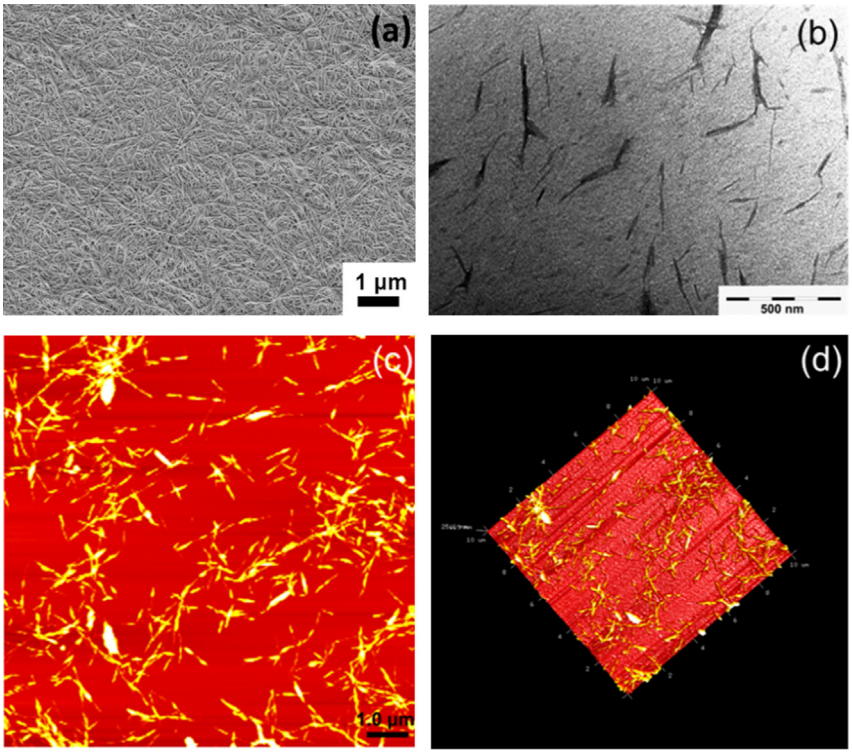

Fig. 2. SEM (a), TEM (b), AFM phase (c) and 3D-height (d) images of CNCs.

Table 2
Zeta-potentials of different CNCs aqueous suspensions.

Sample	CNCs	Chitosan-CNCs	Chitosan-CNCs + KPS
Zeta potential (mV)	+37.9	+50.2	+22.0

attributed to the increased positive charge of the CNC suspension conferred by chitosan. As shown in Table 2, the zeta potential of the chitosan-CNC suspension was much higher than that of the CNC suspension. As expected, adding KPS decreased the zeta potential of the chitosan-CNC suspension (+22.0 mV). A positively charged chitosan-CNC suspension guarantees the stability of the suspension upon the addition of KPS. The mechanism by which the chitosan and CNCs interact is shown in Fig. 5. PAAm-CNCs NC gels with good mechanical properties can be successfully synthesized by adding the interfacial modifier chitosan.

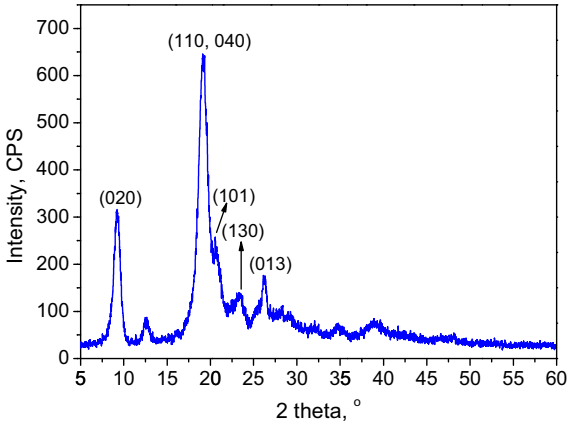

Fig. 3. XRD patterns of the CNCs.

3.3. Mechanical properties of PAAm-CNCs NC gels

Load-bearing applications of hydrogels, such as their use as engineering devices, are often limited by their low mechanical strength. Several approaches have been used to improve the mechanical performance of hydrogels, including using double networks [36,37] and the incorporation of nanoparticles. The appearances of pure PAAm and PAAm-CNCs NC gels are shown in Fig. 6. The PAAm hydrogel is transparent, while the NC gels become translucent due

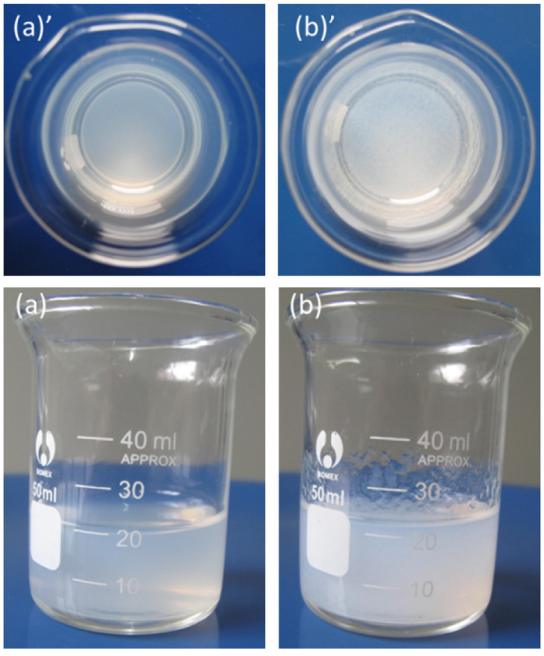

Fig. 4. Photos of CNCs suspension before (a) and after (b) adding of KPS.

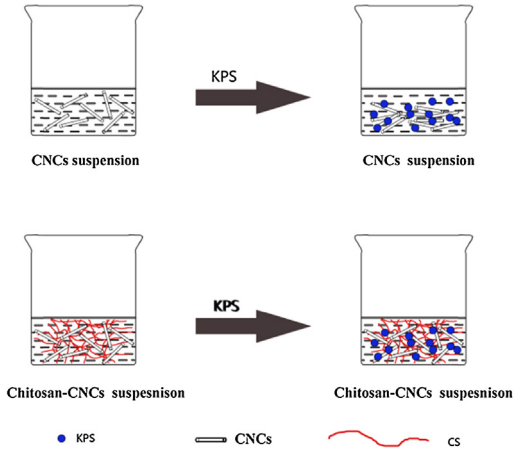

Fig. 5. Schematics shows the changes of CNCs and chitosan-CNCs suspensions by addition of KPS.

to the CNCs. The PAAm hydrogel was very brittle and readily broke upon stretching. The PAAm-CNCs NC gels were tough and could be extensively stretched and even knotted (Fig. 6(e) and (f)). The mechanical stress could transfer from the flexible polymer matrix to the rigid CNCs network. Because uniform NC gels were obtained without the use of organic cross-linkers, the CNCs act as physical cross-linkers for PAAm chains via interfacial hydrogen bond interactions between the amide side groups on the polymer and the surfaces of the CNCs (hydroxyl and amino groups) [20].

To investigate the influence of CNCs on the mechanical performances of PAAm, the prepared hydrogels were subjected to tensile testing using a universal mechanical properties testing machine. The NC gels featured ultrahigh extensibility and could uniformly deform in response to a tensile force without necking, which was attributed to the low chain density and amorphous structure of the gels (Fig. 7(a–c)). The NC gel recovered a large proportion of elongation when broken. Fig. 7(d) shows the tensile stress–strain curves of NC gels. The tensile strength and elongation at break (ε_b) of the linear PAAm were very low. The incorporation of only CNCs slightly improved the tensile properties of the PAAm-CNCs hydrogel (PW), which was attributed to the aggregation of the CNCs in the hydrogel, as shown in Fig. 4(b). Further increasing the loading of CNCs in the hydrogels increased the tensile strength but slightly decreased the elongation. The maximum tensile strength and ε_b of the NC gels were 90 kPa and 3070%, respectively. The area below the tensile stress–strain curve represents the fracture energy of the materials. The PWC and $PW_{1.85}C$ gels were significantly tougher than the PC, PW, and PAAm. The "PW1.85C" demonstrates that the weight ratio of CNCs and chitosan in the NC gels was 1.85:1. The tensile strength of the prepared NC gels is also much larger than the reported traditional PAAm hydrogels crosslinked by organic reagents (i.e., N,N′-methylenebisacrylamide) whose tensile strength is only 14 kPa [24]. The appearances of the highly stretchable NC gels before, during, and after tensile testing are shown Fig. 7(a)–(c). In the PC hydrogel (only chitosan was incorporated into the PAAm), there is absence of a crosslinker; so they formed a very viscous, sticky, gel-like material. The PC hydrogel could be irreversibly elongated extensively (more than 4000%) at very low stress (~10 kPa). This is because PAAm has a high molecular weight and forms a lightly, self-crosslinked network, including topological entanglements [20]. Therefore, the incorporation of chitosan and CNCs synergistically reinforced the PAAm hydrogel.

The excellent mechanical properties of the prepared NC gel, such as the high ε_b (~3100%) and high tensile strength (~90 kPa), are superior or comparable to previously reported results. Sun et al. prepared double network hydrogels composed of ionically crosslinked alginate and covalently crosslinked polyacrylamide. Although the fracture energies of the prepared hydrogels was as high as 9000 J m^{-2}, they could only be stretched to ~20 times their initial length (2000%) [36]. The maximum elongation ratio of polyacrylic acid-cellulose nanocrystals NC gels was only 1100%, while the tensile strength of this formulation was ~100 kPa [38]. Graphene oxide (GO) could effectively increase the tensile properties of PAAm; the PAAm-GO NC gels exhibited a maximum tensile strength and elongation at break of 385 kPa and 3435%, respectively [25]. The elongation at break of the PAAm-CNCs NC gels studied herein is comparable to that of the PAAm-GO NC gels, but the former were much weaker than the latter. The low strength is mainly attributed to the low AM monomer content in the same volume of hydrogel. For example, 5.4 g of AM was used in 20 mL of water to prepare the PAAm-GO hydrogel, while only 3 g of AM was used in 20 mL of water to prepare the PAAm-CNCs hydrogel in the present work. The mechanical properties of the PAAm-CNCs NC gels are comparable to those of PAAm-Laponite NC gels with a similar polymer-to-water ratio. PAAm-Laponite NC gels (2 g of PAAm polymer in 20 mL of water) containing 5% Laponite exhibited a tensile strength and elongation at break of 107 kPa and 2829%, respectively [24]. The tensile performance of the present PAAm-CNCs NC gels was also superior to that of our previously reported PAAm-HNTs NC gel systems [29].

Fig. 7(c) shows that the NC gel sample could recover a large proportion of elongation when broken. The stress–strain curves for the elongation–recovery of the NC gels are shown in Fig. 8. The NC gels were nearly free of residual strain after 1000% or 2000%

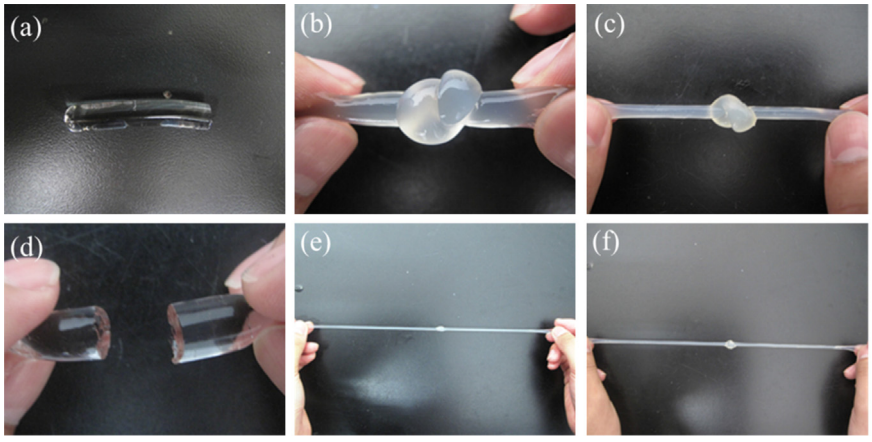

Fig. 6. Appearances of pure PAAm (a), PWC (b), and $PW_{1.85}C$ (c) NC gels and corresponding upon stretching (d, e, f) respectively.

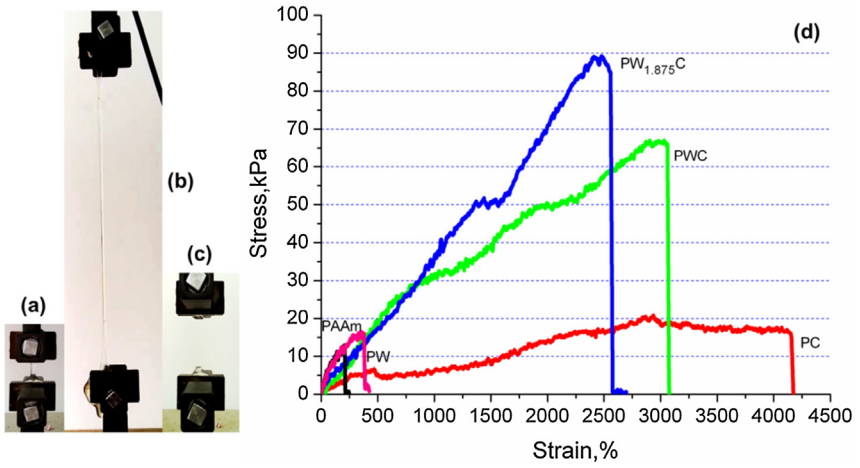

Fig. 7. Stretching processes of the PWC hydrogel during the tensile measurements: (a) the original hydrogel, (b) the hydrogel in elongation, and (c) the hydrogel after elongation. Tensile stress–strain curves for PAAm-CNCs NC gels (d).

elongation. This finding indicates that the good elasticity of the NC gels can effectively dissipate energy. The stress can transfer from the flexible polymer phase to the rigid nanocrystals. Similar to the poly(Nisopropylacrylamide)(PNIPAm)-nanoclay NC gel, the free-radical polymerization of acrylamide was initiated by the redox system close to the surface of CNCs. The dispersed CNCs that feature polymer chains grafted to their surfaces can act as the physical crosslink points for PAAm via this mechanism [20]. Upon loading, the PAAm chains can be completely stretched during tensile testing. When unloading the stress, the NC gels can return to their initial shape and almost entirely avoid permanent deformation. Unlike the covalently crosslinked PAAm hydrogel, the polymer chains anchored to the CNC surfaces via non-covalent interactions can slip along the nanoparticles during the tensile testing. These facts led to the increased strength and extensibility of the NC gels.

3.4. Viscoelastic properties of PAAm-CNCs NC gels

To further investigate the influence of CNCs on the microstructures of the PAAm hydrogel, the dynamic viscoelastic properties were examined with a rotational rheometer. Fig. 9(a) shows the shear modulus (G') curves of the gels as a function of strain. The G' of the NC gels substantially increased upon the incorporation of CNCs. For example, the G' of PWC NC gels at 1% strain was 1043.7 Pa, which was 61% higher than that of the PAAm sample. The value of the G' of linear PAAm was nearly independent of the strain from 0.1% to 30% and slightly decreased beyond this range. The G' of the PWC NC gels sharply decreased when the strain

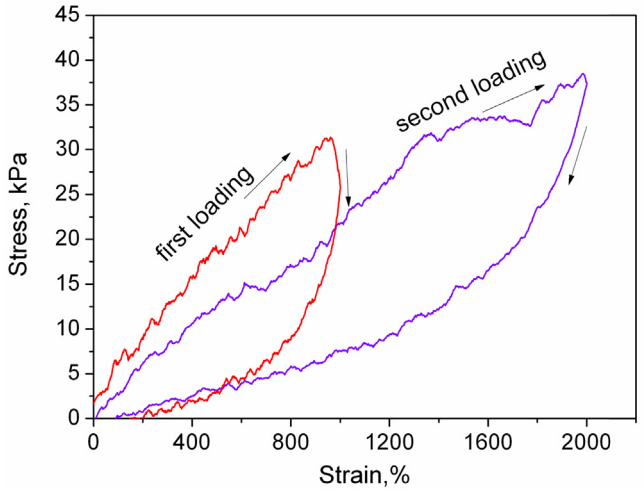

Fig. 8. The stress–strain curves for elongation–recovery of the PWC NC gels.

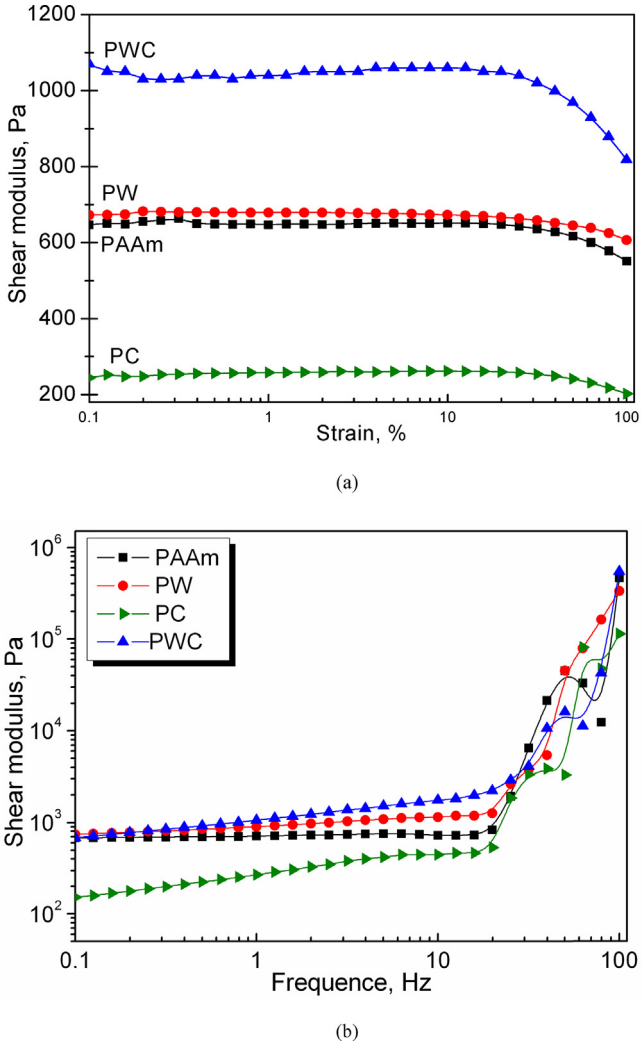

Fig. 9. Strain (a) and angular frequency (b) dependence of storage modulus G' at 25 °C for PAAm and PAAm-CNCs NC gels.

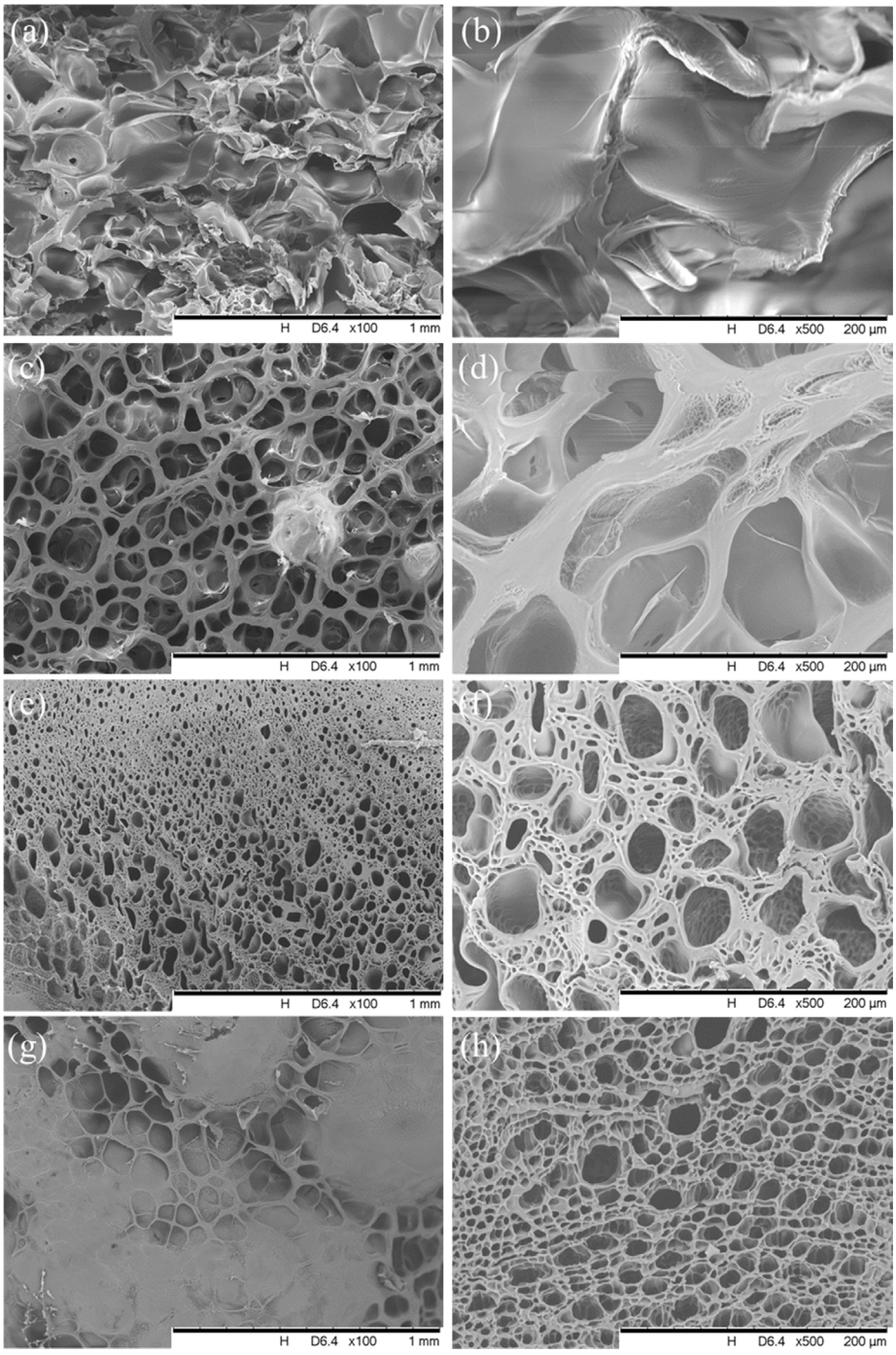

Fig. 10. SEM photos of freeze-dried PAAm-CNCs NC gels: (a) and (b) PAAm; (c) and (d) PW; (e) and (f) PWC; (g) and (h) $PW_{1.85}C$.

exceeded 30%. This difference may arise from the formation of rigid but loose nanofiller networks, which may be seriously damaged by stress [29]. Thus, the G' of the NC gels sharply decreased. The G' of weak PC hydrogel decreased for all strain ranges and was lower than that of the neat PAAm.

Fig. 9(b) compares the angular frequency dependence of G' of the NC gels and linear PAAm. The low frequency did not differ among the PAAm, PW, and PWC samples. Moreover, the G' of the NC gels containing CNC was higher than that of the linear PAAm hydrogel from ~1 to ~30 Hz. Furthermore, the G' of the NC gels depended on the frequency from ~1 to ~30 Hz, while the pure PAAm was nearly frequency independent. The frequency dependence of G' has also been observed for other physically cross-linked hydrogels [39–41], which could be attributed to the following: CNCs may physically interact with the polymer chains via hydrogen bonds, which increases the viscoelastic properties of the hydrogel [41]. Therefore, the G' of the PAAm hydrogel did not depend on the frequency. However, G' sharply increased at high frequencies for all samples, and differences could not be identified among these samples. Only the bond length and bond angle of polymers can move at high frequencies. CNCs can only affect the network structures of polymers. As a result, the effect of CNCs on the G' is less pronounced at high frequencies than that at low frequencies. Furthermore, the G' of the PC hydrogel was lowest due to lack of the crosslinking structures. Overall, the dynamic rheology analysis further suggested that CNCs effectively reinforced PAAm hydrogels.

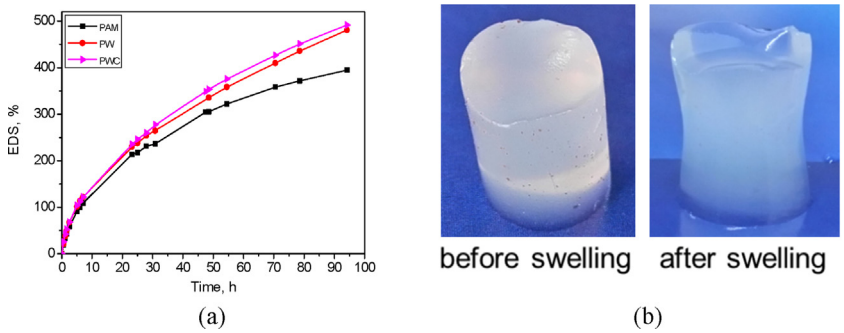

Fig. 11. The equilibrium swelling ratio curves for prepared gels as a function of swelling time (a) and the appearance of PWC gels before and after swelling (b).

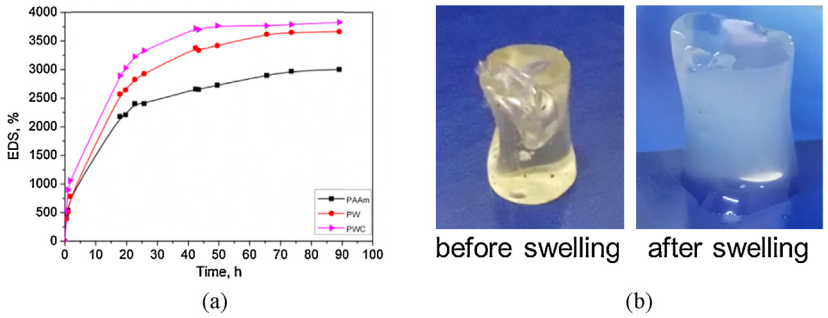

Fig. 12. The equilibrium swelling ratio curves for naturally dried gel samples as a function of swelling time (a) and the appearance of dried PWC gels before and after swelling (b).

3.5. Microstructure of PAAm-CNCs NC gels

Fig. 10 shows the SEM images of the freeze-dried hydrogels. All prepared hydrogels exhibited a porous microstructure with interconnected channels. The pore size of the PAAm hydrogel (~200 μm) markedly decreased upon the incorporation of CNCs. The pores of the PWC and $PW_{1.85}C$ hydrogels were much smaller than those of PAAm and PW. The pores formed via the phase separation during the freeze-drying process. The decreased pore size upon the incorporation of nanoparticles was attributed to the following two facts: the NC gels contained less water than the same volume of PAAm hydrogel. The material (polymer and CNCs) concentration inversely correlated with the pore diameter. The increased crosslinking density and rapid phase separation process by the nanoparticles also resulted in smaller pores in the hydrogel. The CNCs are not easily distinguished in the photos, possibly because they are embedded in the polymer matrix. The high porosity is critical for many hydrogel applications, such as wastewater treatment, tissue engineering, and drug carrier applications.

3.6. Swelling properties of PAAm-CNCs NC gels

To determine the swelling properties, the prepared and naturally dried gels were soaked in a large amount of water. Fig. 11(a) shows the equilibrium swelling ratio curves for different as-prepared gels as a function of the swelling time. The EDS positively correlated with the immersion time for all samples. PAAm hydrogel exhibited the lowest EDS among the samples. Adding CNCs to the PAAm hydrogels increased the EDS due to the hydrophilicity of the CNCs. CNCs contain numerous polar groups that can interact with water via hydrogen bond interactions [42]. The swelling can destroy the superior mechanical properties of the NC gels due to the broken of the hydrogen bonding by the water molecules. The appearances before and after PWC swelling are shown in Fig. 11(b). A similar trend was identified for the dried samples (Fig. 12(a)), but the swelling ratio was much higher. The PWC dried gel swelled more in water than PW and PAAm, which is also due to the increased hydrophilicity of the PAAm hydrogels conferred by the CNCs. The highest EDS of the PWC hydrogel reached 3800%; in other words, this material could absorb 38 times its weight in water. The appearances of the dried PWC before and after swelling are shown in Fig. 12(b). The swelling properties of hydrogels are well known to mainly depend on the hydrophilicity of the functional groups and the effective cross-linking density of the hydrogels. Nanoparticles may increase the cross-linking density of the PAAm hydrogels, which can decrease the swelling ratio [29,43]. Nevertheless, the CNCs are hydrophilic and contain many polar groups, such as —OH and $—NH_2$, which increase the swelling ability of the NC hydrogels. Overall, the prepared NC gels can uptake large amounts of water, which makes them applicable as super-absorbent materials.

4. Conclusions

CNCs synthesized by acidolysis show a high aspect ratio with a uniform width of 10–20 nm and a length of 100–500 nm. Chitosan-CNC suspensions with a high zeta potential value ensure the uniform dispersion of CNCs in the KPS and acrylamide solutions. The chitosan-modified CNCs were used as physical crosslinkers of PAAm to form NC gels. The maximum tensile strength and ε_b of the NC gels were 90 kPa and 3070%, respectively. The shear modulus of the NC gels was significantly higher than that of the PAAm. The microstructures of all hydrogels were porous, but the pores of NC gels were smaller. The maximum swelling equilibrium percentage of the NC gel was 3800%, suggesting their high absorption ability. The changes in the mechanical properties are attributed to the unique structures of CNCs and the interfacial interactions between CNCs and PAAm. The novel PAAm NC gels with CNCs developed in this study may serve a promising absorbent or biomedical material due to the high mechanical properties, high absorb ability of the NC gels and the biological source of CNCs.

Acknowledgements

This work was financially supported by the National Natural Science Foundation of China (grant No. 51473069) and the Guangdong Natural Science Funds for Distinguished Young Scholars (grant No. S2013050014606).

References

[1] R.H. Marchessault, F.F. Morehead, N.M. Walter, Nature 184 (1959) 632–633.
[2] L. Heath, L. Zhu, W. Thielemans, Chem. Sus. Chem. 6 (2013) 537–544.
[3] M. Mincea, A. Negrulescu, V. Ostafe, Rev. Adv. Mater. Sci. 30 (2012) 225–242.
[4] J.B. Zeng, Y.S. He, S.L. Li, Y.Z. Wang, Biomacromolecules 13 (2012) 1–11.
[5] K.G. Nair, A. Dufresne, A. Gandini, M.N. Belgacem, Biomacromolecules 4 (2003) 1835–1842.
[6] K.G. Nair, A. Dufresne, Biomacromolecules 4 (2003) 657–665.
[7] K.G. Nair, A. Dufresne, Biomacromolecules 4 (2003) 666–674.
[8] P.M. Visakh, M. Monti, D. Puglia, M. Rallini, C. Santulli, F. Sarasini, S. Thomas, J.M. Kenny, Express Polym. Lett. 6 (2012) 396–409.
[9] A. Saralegi, S.C.M. Fernandes, A. Alonso-Varona, T. Palomares, E.J. Foster, C. Weder, A. Eceiza, M.A. Corcuera, Biomacromolecules 14 (2013) 4475–4482.
[10] M. Paillet, A. Dufresne, Macromolecules 34 (2001) 6527–6530.
[11] Y.S. Lu, L.H. Weng, L.N. Zhang, Biomacromolecules 5 (2004) 1046–1051.
[12] X.X. Li, X.Y. Li, B.L. Ke, X.W. Shi, Y.M. Du, Carbohydr. Polym. 85 (2011) 747–752.
[13] J. Sriupayo, P. Supaphol, J. Blackwell, R. Rujiravanit, Polymer 46 (2005) 5637–5644.
[14] A.J. Uddin, M. Fujie, S. Sembo, Y. Gotoh, Carbohydr. Polym. 87 (2012) 799–805.
[15] Y. Huang, L.N. Zhang, J. Yang, X.Z. Zhang, M. Xu, Macromol. Mater. Eng. 298 (2013) 303–310.
[16] P. Wongpanit, N. Sanchavanakit, P. Pavasant, T. Bunaprasert, Y. Tabata, R. Rujiravanit, Eur. Polym. J. 43 (2007) 4123–4135.
[17] R. Xiong, C. Lu, W. Zhang, Z. Zhou, X. Zhang, Carbohydr. Polym. 95 (2013) 214–219.
[18] X. Wu, C. Lu, W. Zhang, G. Yuan, R. Xiong, X. Zhang, J. Mater. Chem. A 1 (2013) 8645–8652.
[19] K. Haraguchi, T. Takehisa, Adv. Mater. 14 (2002) 1120–1124.
[20] K. Haraguchi, Polym. J. 43 (2011) 223–241.
[21] K. Haraguchi, T. Takehisa, S. Fan, Macromolecules 35 (2002) 10162–10171.
[22] K. Haraguchi, M. Ebato, T. Takehisa, Adv. Mater. 18 (2006) 2250–2254.
[23] L. Xiong, M. Zhu, X. Hu, X. Liu, Z. Tong, Macromolecules 42 (2009) 3811–3817.
[24] M.F. Zhu, Y. Liu, B. Sun, W. Zhang, X.L. Liu, H. Yu, Y. Zhang, D. Kuckling, H.J.P. Adler, Macromol. Rapid Commun. 27 (2006) 1023–1028.
[25] R.Q. Liu, S.M. Liang, X.Z. Tang, D. Yan, X.F. Li, Z.Z. Yu, J. Mater. Chem. 22 (2012) 14160–14167.
[26] C. Zhou, Q. Wu, Y. Yue, Q. Zhang, J. Colloid Interface Sci. 353 (2011) 116–123.
[27] J. Yang, C.-R. Han, J.-F. Duan, M.-G. Ma, X.-M. Zhang, F. Xu, R.-C. Sun, Cellulose 20 (2013) 227–237.
[28] R. Liu, S. Liang, X.-Z. Tang, D. Yan, X. Li, Z.-Z. Yu, J. Mater. Chem. 22 (2012) 14160–14167.
[29] M. Liu, W. Li, J. Rong, C. Zhou, Colloid. Polym. Sci. 290 (2012) 895–905.
[30] S. Ifuku, M. Nogi, K. Abe, M. Yoshioka, M. Morimoto, H. Saimoto, H. Yano, Biomacromolecules 10 (2009) 1584–1588.
[31] Y. Lu, Q. Sun, X. She, Y. Xia, Y. Liu, J. Li, D. Yang, Carbohydr. Polym. 98 (2013) 1497–1504.
[32] H.-P. Zhao, X.-Q. Feng, H. Gao, Appl. Phys. Lett. 90 (2007) 073112.
[33] Y. Fan, T. Saito, A. Isogai, Biomacromolecules 9 (2008) 1919–1923.
[34] Y.-W. Cho, J. Jang, C.R. Park, S.-W. Ko, Biomacromolecules 1 (2000) 609–614.
[35] X. Zhao, Z. Xu, Y. Xie, B.N. Zheng, L. Kou, C. Gao, Langmuir 30 (2014) 3715–3722.
[36] J.Y. Sun, X.H. Zhao, W.R.K. Illeperuma, O. Chaudhuri, K.H. Oh, D.J. Mooney, J.J. Vlassak, Z.G. Suo, Nature 489 (2012) 133–136.
[37] J. Li, W.R.K. Illeperuma, Z. Suo, J.J. Vlassak, ACS Macro Lett. 3 (2014) 520–523.
[38] J. Yang, C.R. Han, J.F. Duan, M.G. Ma, X.M. Zhang, F. Xu, R.C. Sun, X.M. Xie, J. Mater. Chem. 22 (2012) 22467–22480.
[39] H.J. Kong, E. Wong, D.J. Mooney, Macromolecules 36 (2003) 4582–4588.
[40] K.J. Jeong, A. Panitch, Biomacromolecules 10 (2009) 1090–1099.
[41] C.-J. Wu, A.K. Gaharwar, B.K. Chan, G. Schmidt, Macromolecules 44 (2011) 8215–8224.
[42] A. Villares, C. Moreau, I. Capron, B. Cathala, Biomacromolecules 15 (2013) 188–194.
[43] C. Zhou, Q. Wu, Colloids Surf. B 84 (2011) 155–162.